The magnetic properties of (La,Ce)Co$_5$ ((La,Ce)=La$_{0.35}$Ce$_{0.65}$, La-Ce mischmetal) nanoflakes prepared by surfactant-assisted ball milling

X. Zhao, W. L. Zuo, D. Liu, J. F. Xiong, S. L. Zuo, Y. Zhang, X. Q. Zheng, F. X. Hu, T. Y. Zhao, J. R. Sun, and B. G. Shen

---

CrossMark
←click for updates

The magnetic properties of (La,Ce)Co$_5$ ((La,Ce)=La$_{0.35}$Ce$_{0.65}$, La-Ce mischmetal) nanoflakes prepared by surfactant-assisted ball milling

X. Zhao,[1,2] W. L. Zuo,[1,3] D. Liu,[1,2] J. F. Xiong,[1,2] S. L. Zuo,[1,2] Y. Zhang,[1,2] X. Q. Zheng,[1,4] F. X. Hu,[1,2] T. Y. Zhao,[1,2] J. R. Sun,[1,2] and B. G. Shen[1,2,a]

[1]*State Key Laboratory of Magnetism, Institute of Physics, Chinese Academy of Sciences, Beijing 100190, PR China*
[2]*University of Chinese Academy of Sciences, Beijing 100049, PR China*
[3]*School of Science, Xi'an Jiaotong University, Xi'an 710049, PR China*
[4]*School of Materials Science and Engineering, University of Science and Technology Beijing, Beijing 100083, PR China*

The hard magnetic (La,Ce)Co$_5$ nanoflakes with high coercivity and narrow thickness distribution have been successfully obtained by surfactant-assisted ball milling (SABM). The magnetic properties, morphology and interaction of (La,Ce)Co$_5$ nanoflakes are studied in this work. The coercivity and remanence ratio of (La,Ce)Co$_5$ nanoflakes are 5.48 kOe and 0.71, respectively. The X-ray powder diffraction (XRD) patterns indicate that the (La,Ce)Co$_5$ nanoflakes are CaCu$_5$-type hexagonal crystal structure. The average thickness and aspect ratio are 47 nm and 40, respectively. The intergrain interaction of the (La,Ce)Co$_5$ nanoflakes is studied using the $\delta m(H)$-curves technique which shows the magnetostatic-dominated particle interaction. The high coercivity and narrow thickness distribution of (La,Ce)Co$_5$ nanoflakes could be promising for the future development of the high performance soft/hard exchange spring magnets. © *2017 Author(s). All article content, except where otherwise noted, is licensed under a Creative Commons Attribution (CC BY) license (http://creativecommons.org/licenses/by/4.0/).* https://doi.org/10.1063/1.5007209

INTRODUCTION

Recently, Co-based rare earth permanent magnetic compounds with high coercivity and high operation temperature have drawn much attention due to they can be used for obtaining high performance nanocomposite magnets and soft/hard exchange coupled magnets.[1–6] Many Co-based rare earth permanent magnetic nanoflakes or nanoparticles have been prepared by the ball milling (BM) method, which are promising materials for preparing the high-performance nanostructured permanent magnets.[7] In order to decrease the defects from BM and crush the sample into a smaller size especially for a nanoscaled size, SABM experiments are carried out for preparing nanostructured magnetic materials, and obtaining excellent magnetic properties. Nevertheless, most of the experiments are based on the rare earth elements of Sm or Pr,[7,8] which are expensive for application. In our previous work, the high performance MMCo$_5$ (MM=mischmetal) nanoflakes have been successfully obtained.[9] Furthermore, we hope the (La,Ce)Co$_5$ nanoflakes can also show the excellent permanent magnetic properties because of the purification and separation of mischmetal lead a large surplus of La and Ce elements and the use of La-Ce mischmetal would also play a positive role in the balanced utilization of rare earths. In this work, we prepared the (La,Ce)Co$_5$ nanoflakes by SABM and studied these room-temperature magnetic properties.

---

[a]Corresponding author: shenbaogen@yeah.net

EXPERIMENT

The (La,Ce)Co$_5$ ingots were obtained by arc-melting in argon atmosphere using pure metals Co (99.99 wt. %) and La-Ce mischmetal (98 wt. %) with 2 wt. % excess for the evaporation losses. The atom ratio of (La,Ce) and Co was 1:5. The ingots were melted five times to ensure homogeneity and then annealed at 1173 K for 5 days under vacuum. The (La,Ce)Co$_5$ ingots were manually crushed and then grounded down to less than 400 μm as the coarse powders.[7,9] Oleylamine (85 %) and oleic acid (99 %) was used as surfactant (the volume ratio of Oleylamine and oleic acid was 1:1) and heptane (99 %) was used as the carrier liquid. We put the stainless steel balls, coarse powders (the mass of about 5 g), surfactant and carrier liquid into the milling vial. The total amount of surfactant was about 20 % to the weight of the coarse powders. To prevent oxidation, all of these operations were done in an argon-filled glove box. The SABM experiment was performed with a GN-2 high-energy ball miller with the milling energy of 300 rpm (the voltage was about 60 V). The (La,Ce)Co$_5$ nanoflakes/resin composite was prepared by mixing the as-milled slurry with epoxy resin (about 2 mg of (La,Ce)Co$_5$ nanoflakes mixed with at least 200 mg of epoxy resin) in argon-filled glove box. After the epoxy resin solidified, we cut strips (about 2 mm long, 1 mm wide and 0.5 mm thick) from the composite for the following analysis.[8,9] The phase structure was examined by the X-ray powder diffraction (XRD) (Rigaku D/Max-2400) with Cu K$_\alpha$ radiation at room temperature. Morphology was characterized by scanning electron microscope (SEM) (XL30S-FEG). Magnetic properties were measured by SQUIDVSM (MPMS-3 Quantum Design) with the maximum field of 70 kOe.

RESULTS AND DISCUSSION

Fig. 1 shows the magnetic hysteresis loops, remanence ratio (Mr/Ms) and coercivity of (La,Ce)Co$_5$ nanoflakes after ball milled from 5 h to 9 h with the milling energy was 300 rpm. The coercivity increases at first, because the continuous grain refinement yields many grain boundaries and residual stresses in the nanoflakes, which acts as pinning sites for domain wall motion. When the ball milling time reached to 8 h, the coercivity increased to the maximum value of 5.48 kOe. After that, the coercivity decreases slowly. Compared with the coercivity, the remanence ratio Mr/Ms shows monotonically decreased. Surfactant plays a crucial role to prevent the close contact of the fine particle by providing steric barrier, and it could lower the energies of freshly form fine particle surface by forming a thin organic layer around the nanoflakes. Surfactant can lower the energies of freshly cleaved surfaces, enable long-range capillary forces, impede cold welding and the agglomeration and lower the energy required for crack propagation.[10,11] The reduction of brittleness and increment of
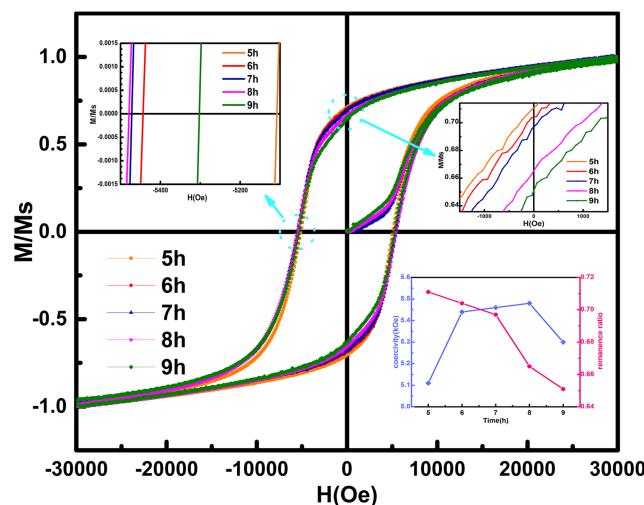

FIG. 1. The magnetic hysteresis loop, remanence ratio (Mr/Ms) and coercivity of (La,Ce)Co$_5$ nanoflakes after ball milled from 5 h to 9 h with the milling energy was 300 rpm, respectively.
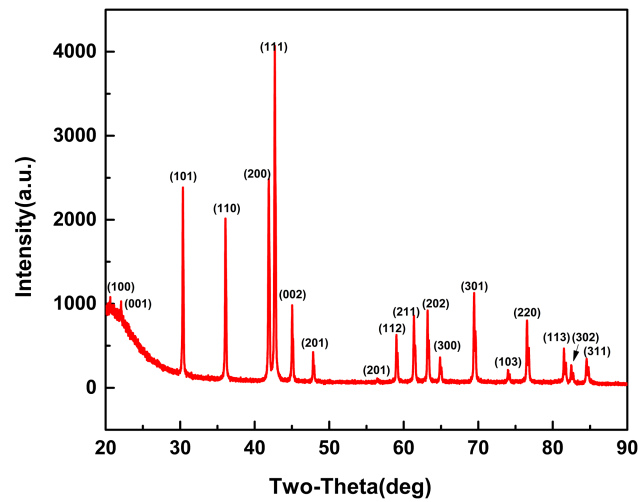
FIG. 2. The XRD patterns of randomly oriented (La,Ce)Co5 coarse powders and the direction are shown near the peaks.

ductility leads to the decrease of grain refinement efficiency when the particle size approached into nanocrystalline structure, which leads coercivity declined.[11,12] The other reason of the decline of coercivity is that BM leads to partial amorphorization and smaller particles with a more amorphous structure leads to the reduced of coercivity.[12]

Fig. 2 shows the XRD pattern of randomly oriented coarse $(La,Ce)Co_5$ powders it can be seen that the main phase crystal in $(La,Ce)Co_5$ is $CaCu_5$-type hexagonal structure (the space group is P6/mmm). It can be seen that hardly any rare-earth oxides or impurity peak appeared, which indicates that the prepared nanoflakes have been effectively protected from oxidation during the fabrication and examination processes.

Fig. 3 shows the morphology evolution of $(La,Ce)Co_5$ nanoflakes with different SABM time. From Fig. 3A–3E we can see that when the experiment performed with the milling energy of 300 rpm, the thickness of nanoflakes reach to the critical dimension of magnetic domain of $(La,Ce)Co_5$ which was about 2 μm.[9] With the experiment performed after 8 h, the structure of magnetic domain was destructed, which might lead the decrease of coercivity. Because of the increment of small poly-crystalline nanoflakes, the random orientation incline and the grain boundaries turn incoherence. The
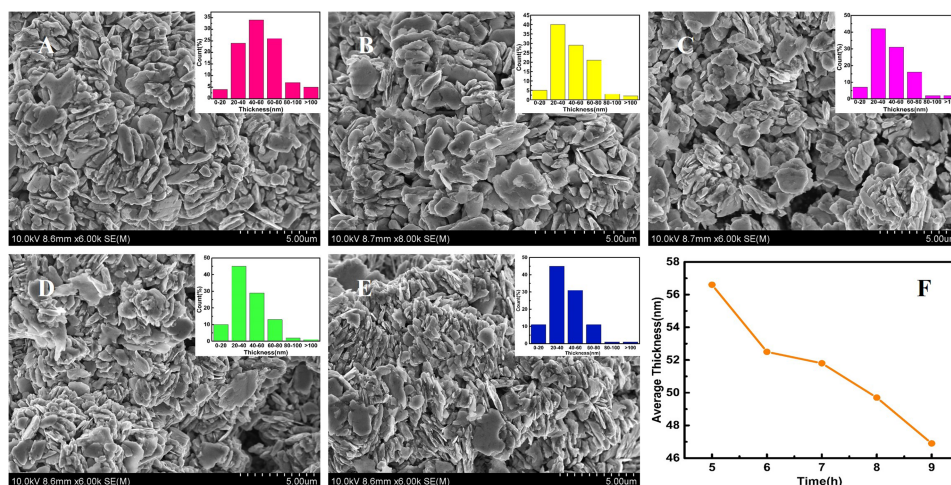

FIG. 3. A-3E The SEM images of $(La,Ce)Co_5$ nanoflakes with different SABM time from 5 h to 9 h. The insets show the distribution of grain size performed in every stages. Fig. 3F The average thickness of $(La,Ce)Co_5$ nanoflakes obtained by SABM with different time.
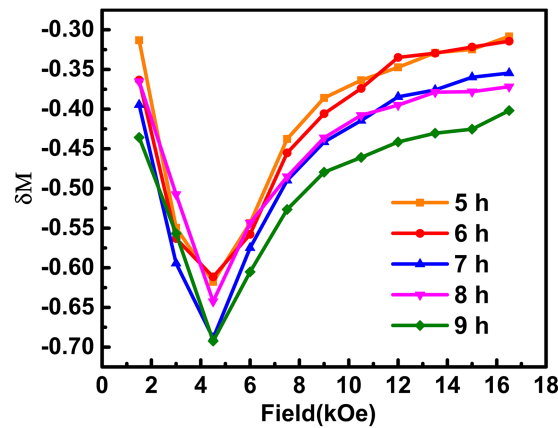
FIG. 4. The $\delta m(H)$-curves of (La,Ce)Co$_5$ nanoflakes after ball milled from 5 h to 9 h with the milling energy was 300 rpm.

decrease of Mr/Ms also indicates that the high energy was harmful for forming textured nanoflakes. The (La,Ce)Co$_5$ sample is brittle and easily crushed, after ball milling 5 h with the milling energy of 300 rpm, the coarse powders were crushed down to smaller nanoflakes with the average thickness of 57 nm and in-plane size of about 2 μm. With prolonging milling time up to 8 h, the nanoflakes become relative uniformity nanoflakes with thickness of 50 nm. Compared with Fig. 1, we can see that when the thickness is about 50 nm (from 50 nm to 52 nm), the coercivity reach to maximum. In addition, an obvious "kebab-like" morphology forms with the submicro-flakes due to the c-axis textured and magnetostatic interaction or dipolar coupling. The insets of Fig. 3 show the distribution of grain size performed in every stages. With the milling was going on, the thickness distribution of nanoflakes was increasingly concentrated. The thickness distribution is asymmetric normal distribution, the thicker nanoflakes are much more than the thinner. With the experiment continued, the distribution of thickness nanoflakes is more and more centralized.

In a real magnet, the relation between isothermal remanence $M_r(H)$ and demagnetization remanence $M_d(H)$ is expressed as $\delta m(H) = [M_d(H) - M_r(\infty) + 2M_r(H)] / M_r(\infty)$.[13] Here $M_d(H)$ is the dc demagnetization remanence and can be obtained by saturating the sample in one direction followed by subsequent application and removal of the applied field in the reverse direction. The other term $M_r(H)$ is known as the isothermal remanent magnetization and can be measured experimentally by starting with a fresh sample and consequent application and removal of the applied field in one direction. The procedure has to be continued until the magnetic saturation of the sample for the measurement of $M_d(\infty)$.[14] It is believed that nonzero δm is due to the interactions between particles in the magnet. The positive value of δm is primarily caused by intergrain exchange coupling, while the negative value of δm is primarily caused by magnetostatic interaction.[13–15] From Fig. 4 we can see that the value of δm is negative in all stages, which means the magnetostatic-dominated particle interaction. In the same external magnetic field, the value of δm decreased with the milling continued. Because when the field H is near coercivity H_c, the project of total moment of magnet to field direction is zero, a peak appeared near the coercivity. Because the nanoflakes might orientate before the epoxy resin solidified, the position of peak is smaller than the coercivity.

CONCLUSIONS

The low cost (La,Ce)Co$_5$ nanoflakes with large coercivity of 5.48 kOe and high remanence ratio of 0.71 were obtained by SABM with the heat-treated coarse powder. The SEM results of (La,Ce)Co$_5$ nanoflakes indicate the thickness and in-plane size of ball milled samples are mainly about 50±5 nm and 2 μm, respectively. The XRD results of (La,Ce)Co$_5$ indicated the nanoflakes are CaCu$_5$-type hexagonal crystal structure. The (La,Ce)Co$_5$ nanoflakes with large coercivity and low cost are very promising for the building blocks for the future high-performance nanocomposite permanent magnets with an enhanced energy product.

ACKNOWLEDGMENTS

[1] S. H. Sun, C. B. Murray, D. Weller, L. Folks, and A. Moser, Science **287**, 1989 (2000).

[2] H. Zeng, J. Li, J. P. Liu, Z. L. Wang, and S. Sun, Nature **420**, 395 (2002).

[3] N. G. Akdogan, G. C. Hadjipanayis, and D. J. Sellmyer, IEEE. Trans. Magn. **45**, 4417 (2009).

[4] M. Yue, Y. P. Wang, N. Poudyal, C. B. Rong, and J. P. Liu, J. Appl. Phys. **105**, 07A708 (2009).

[5] S. J. Knutson, Y. Shen, J. C. Horwath, P. Barnes, and C. H. Chen, J. Appl. Phys. **109**, 07A762 (2011).

[6] S. K. Pal, L. Schultz, and O. Gutfleisch, J. Appl. Phys. **113**, 013913 (2013).

[7] W. L. Zuo, R. M. Liu, X. Q. Zheng, R. R. Wu, F. X. Hu, J. R. Sun, and B. G. Shen, J. Appl. Phys **115**, 17A728 (2014).

[8] W. L. Zuo, X. Zhao, J. F. Xiong, M. Zhang, T. Y. Zhao, F. X. Hu, J. R. Sun, and B. G. Shen, Sci. Rep. **5**, 13117 (2015).

[9] X. Zhao, W. L. Zuo, M. Zhang, D. Liu, J. F. Xiong, R. X. Shang, J. Zhang, T. Y. Zhao, J. R. Sun, and B. G. Shen, AIP Adv. **7**, 056203 (2017).

[10] S. K. Pal, L. Schultz, and O. Gutfleisch, Scri. Mat. **33**, 1359 (2014).

[11] N. Poudyal, C. B. Rong, and J. P. Liu, J. Appl. Phys. **107**, 09A703 (2010).

[12] Y. P. Wang, Y. Li, C. B. Rong, and J. P. Liu, Nanotechnology **18**, 465701 (2007).

[13] H. W. Zhang, C. B. Rong, X. B. Du, J. Zhang, S. Y. Zhang, and B. G. Shen, Appl. Phys. Letters **82**, 4098 (2003).

[14] D. Roy and P. S. Anil Kumar, J. Appl. Phys. **106**, 073902 (2009).

[15] Q. Chen, B. M. Ma, B. Lu, M. Q. Huang, and D. E. Laughlin, J. Appl. Phys. **85**, 5917 (1999).